Chem. Senses 33: 201–210, 2008
doi:10.1093/chemse/bjm079
Advance Access publication January 8, 2008

Sensory Deafferentation Transsynaptically Alters Neuronal GluR1 Expression in the External Plexiform Layer of the Adult Mouse Main Olfactory Bulb

Kathryn A. Hamilton[1], Stephanie Parrish-Aungst[2], Frank L. Margolis[2], Ferenc Erdélyi[3], Gabor Szabó[3] and Adam C. Puche[2]

[1]Department of Cellular Biology and Anatomy, Louisiana State University Health Sciences Center, 1501 Kings Highway, Shreveport, LA 71130-3932, USA, [2]Department of Anatomy and Neurobiology and Program in Neuroscience, University of Maryland, Baltimore, MD 21201, USA and [3]Department of Gene Technology and Developmental Neurobiology, Institute of Experimental Medicine, Budapest, Hungary

Correspondence to be sent to: Kathryn Hamilton, Department of Cellular Biology and Anatomy, Louisiana State University Health Sciences Center, 1501 Kings Highway, Shreveport, LA 71130-3932, USA. e-mail: khamil@lsuhsc.edu

Abstract

Altered distribution of the alpha-amino-3-hydroxy-5-methylisoxazole-4-propionic acid (AMPA) receptor subunit GluR1 has been linked to stimulation-dependent changes in synaptic efficacy, including long-term potentiation and depression. The main olfactory bulb (OB) remains plastic throughout life; how GluR1 may be involved in this plasticity is unknown. We have previously shown that neonatal naris occlusion reduces numbers of interneuron cell bodies that are immunoreactive for GluR1 in the external plexiform layer (EPL) of the adult mouse OB. Here, we show that immunoreactivity of mouse EPL interneurons for GluR1 is also dramatically reduced following olfactory deafferentation in adulthood. We further show that expression of glutamic acid decarboxylase (GAD) 65, 1 of 2 GAD isoforms expressed by adult gamma-aminobutyric acidergic interneurons, is reduced, but to a much smaller extent, and that in double-labeled cells, immunoreactivity for the Ca^{2+}-binding protein parvalbumin (PV) is also reduced. In addition, GluR1 expression is reduced in presumptive tufted cells and interneurons that are negative for GAD65 and PV. Consistent with previous reports, sensory deafferentation resulted in little neuronal degeneration in the adult EPL, indicating that these differences were not likely due to death of EPL neurons. Together, these results suggest that olfactory input regulates expression of the GluR1 AMPA receptor subunit by tufted cells that may in turn regulate GluR1 expression by interneurons within the OB EPL.

Key words: AMPA receptor, confocal microscopy, immunohistochemistry, olfaction, optical disector, plasticity

Introduction

Alterations in neurotransmitter and receptor distributions often accompany changes in synaptic efficacy. Understanding the regulatory mechanisms underlying these changes is, therefore, key to understanding the role of synaptic plasticity in normal development. In the glomerular layer (GL) of the main olfactory bulb (OB), expression of some neurotransmitters and receptors during early postnatal development has been shown to be regulated by the glutamatergic synaptic input from olfactory nerve (ON) axon terminals, which excite mitral and tufted cell dendrites within the glomeruli (Ennis et al. 1996, 2007; Aroniadou-Anderjaska et al. 1997; Chen and Shepherd 1997; Giustetto et al. 1997). In addition to mitral/tufted cell dendrites, the GL also contains a large population of dopaminergic periglomerular cells, which receive synapses from ON axon terminals (Toida et al. 2000). Blocking normal airflow by neonatal naris occlusion reduces odor stimulation of the olfactory sensory neurons and results in a reduction of tyrosine hydroxylase (TH) and dopamine expression in periglomerular cells and possibly in some tufted cells (Baker 1990). Periglomerular cells nevertheless express aromatic amino acid decarboxylase and gamma-aminobutyric acid (GABA), indicating that different neurotransmitter phenotypes are differentially sensitive to reduced olfactory input (Stone et al. 1991). Many changes observed following neonatal occlusion are permanent and to some extent can be attributed to stunted development of the OB (Brunjes 1994) and/or to the reduced survival of postnatally generated periglomerular cells and

granule cells (Frazier-Cierpial and Brunjes 1989; Corotto et al. 1994; Fiske and Brunjes 2001; Petreanu and Alvarez-Buylla 2002; Saghatelyan et al. 2005; Mandairon et al. 2006). However, reduced TH expression is also observed following adult naris occlusion (Kosaka et al. 1987; Corotto et al. 1994; Saino-Saito et al. 2004), adult surgical deafferentation (Baker et al. 1984), or lesioning of the adult nasal epithelium with zinc sulfate (Nadi et al. 1981; Kawano and Margolis 1982; Baker et al. 1988; Stone et al. 1991), indicating the reduction is not merely a developmental phenomenon. In mice, zinc sulfate treatment destroys olfactory sensory neurons (Margolis et al. 1974; Matulionis 1975; Harding et al. 1978; Burd 1993) and results in anosmia that lasts at least 30 days (McBride et al. 2003). Thus, TH expression by both neonatal and adult neurons that receive input from the ON appears to be transsynaptically regulated.

In the central nervous system, glutamate receptors of the alpha-amino-3-hydroxy-5-methylisoxazole-4-propionic acid (AMPA) subtype mediate most fast excitatory synaptic transmission. Altered expression of these receptors and of their 4 subunits (GluR1–4) has been linked to stimulation-dependent changes in synaptic efficacy (Bredt and Nicholl 2003; Sprengel 2006). Main OB neurons express significant levels of most AMPA receptor subunits, including GluR1 (Petralia and Wenthold 1992; Montague and Greer 1999; Sassoè-Pognetto and Ottersen 2000; Ennis et al. 2007). We have previously shown that neonatal naris occlusion dramatically reduced numbers of GluR1-immunoreactive (IR) interneuron cell bodies in the external plexiform layer (EPL) (Hamilton and Coppola 2003). Because EPL interneurons do not receive direct synaptic input from ON axon terminals, the reduced GluR1 expression presumably resulted from transsynaptic effects of naris occlusion on mitral/tufted cells. Support for this hypothesis derives from ultrastructural studies showing that mitral/tufted cells form excitatory synapses onto the parvalbumin (PV)-IR interneurons of the EPL (Toida et al. 1994, 1996; Crespo et al. 2001). Because the early postnatal EPL contains few cell bodies, the reduction in GluR1-IR could partly be due to failure of developing interneurons to migrate into the EPL (Kosaka et al. 1994b; Hamilton and Coppola 2003). Accelerated death of postnatally generated interneurons could also be a contributing factor because neonatal naris occlusion increases apoptosis in all OB layers. However, the magnitude of increased apoptosis is smaller in the EPL than in other layers (~5% in the EPL + GL relative to the GL alone; Fiske and Brunjes 2001), suggesting cell death does not play a major role. In adults, only ~2% of EPL cells (neurons and glial cells) are generated after postnatal day 20 (Bayer 1983), and only ~7% of adult-generated interneurons derived from the subventricular zone are destined for the EPL (Luskin 1993). Most adult-generated interneurons are instead destined for the granule cell layer (GCL) and to a lesser extent for the GL (Kaplan et al. 1985; Lois and Alvarez-Buylla 1994; Kato et al. 2000; De Marchis et al. 2001, 2007; Wichterle et al. 2001; Takei et al. 2002; Ninkovic et al. 2007). Recent studies show that PV-IR interneurons of the adult mouse EPL do not exhibit significant turnover (Young et al. 2007). Thus, it is unlikely that loss of adult-generated interneurons could be responsible for any reduction in adult GluR1-IR cell bodies.

Here, we show that immunoreactivity of EPL interneurons for GluR1 is dramatically reduced in adult mice following zinc sulfate treatment in adulthood. Expression of glutamic acid decarboxylase (GAD) 65, 1 of 2 GAD isoforms expressed by adult GABAergic interneurons, and immunoreactivity for PV are also reduced in the interneuron population. We further provide evidence suggesting that GluR1 is reduced in GAD65- and PV-negative presumptive tufted cells and interneurons. Together, these results suggest that in the OB EPL, expression of an AMPA receptor subunit and markers typically expressed by inhibitory interneurons are transsynaptically regulated by the excitatory olfactory sensory input to mitral/tufted cells.

Experimental procedures

Animals

Adult mice of both sexes (N = 13) were used in accordance with institutional and National Institutes of Health guidelines. Transgenic mice expressing green fluorescent protein (GFP) under control of the mouse GAD 65-kDa promoter (GAD65-GFP) originally generated by Erdélyi et al. (2002) were obtained from a colony maintained at the University of Maryland, Baltimore, MD. Adult CD-1 mice were obtained from Charles River Laboratories (Wilmington, MA). Previous studies have provided evidence that expression of the GAD65-GFP transgene is a reliable marker for GAD65 protein expression (López-Bendito et al. 2004).

Zinc sulfate lesion

The right naris of GAD65-GFP mice was lavaged with 0.1 cc of either 0.17 M zinc sulfate or 0.01 M Na^+ phosphate buffer + 0.9% NaCl (PBS), as a control treatment. In mice, this procedure effectively lavages the entire nasal cavity, and both cavities are lavaged, due to passage of solution through the window in the nasal septum. Twenty days after treatment, mice were deeply anesthetized with Na^+ pentobarbital (i.p.) and transcardially perfused with 0.9% NaCl followed by freshly prepared 4% paraformaldehyde in PBS, pH 7.4. The brains were embedded in 10% gelatin, and the tissue was cryoprotected and the gelatin was fixed overnight at 4 °C in 30% sucrose in PBS + 1% paraformaldehyde. Eighteen sets of serial coronal sections (25 μm) were obtained using a cryostat and stored at 4 °C.

Staining and imaging

A set of sections from each animal was randomly selected and washed in PBS and nonspecific staining was blocked with

1–2% BSA in 0.1 M Tris buffer containing 0.9% NaCl + 0.3% Triton X-100 (TBST). The sections were then incubated overnight with rabbit anti-GluR1 (1:200, Chemicon/Millipore, Temecula, CA) + mouse anti-PV (1:5000, Swant, Bellinzona, Switzerland) in TBST. Sections incubated in TBST without primary antisera did not exhibit specific labeling. According to the manufacturers, the rabbit anti-GluR1 antiserum was generated against a carboxy terminus peptide of rat GluR1; it was affinity purified using the immunogen, and it does not cross-react with GluR2–4 subunits. The PV antiserum is a monoclonal antiserum that specifically recognizes the ^{45}Ca-binding spot of PV in immunoblot assays.

After washing with TBST, the sections were incubated with biotinylated donkey anti-rabbit IgG (1:500), followed by Cy3-labeled streptavidin (1:500) to label GluR1 and Cy5-labeled donkey anti-mouse IgG (1:500) to label PV; secondary antisera and streptavidin were obtained from Jackson Immunoresearch (West Grove, PA). Other sets of randomly selected sections were incubated for 1 h with Sytox Orange (1:500, Molecular Probes/Invitrogen, Carlsbad, CA), to stain all cells.

The sections were washed and mounted on gelatin-coated slides, and 800 × 600– or 1024 × 768–pixel z-series images (1- to 1.5-μm step size) for each fluorophore were sequentially obtained through the entire thickness of the medial EPL of the right OBs of the middle 3 sections using an Olympus BX51WI microscope and FluoView confocal (Olympus America, Inc., Center Valley, PA) or Nikon TE300 microscope and Bio-Rad Radiance 2000 confocal (Zeiss Microimaging Inc., Thornwood, NY). Because large numbers of cells are stained with Sytox Orange (see Results, Fig. 1d and h), the right bulb of only 1 section (the third) was imaged. A final set of randomly selected sections was labeled with the nuclear stain, TOTO-3 iodide (1:500, Molecular Probes/Invitrogen), and all sections through the right OBs were imaged at low magnification for determining the EPL volume (Parrish-Aungst et al. 2007; see Cell counts, volume measurements, and density estimates). Selected sections were also stained with goat anti-olfactory marker protein (1:25 000), which labels mature olfactory sensory neurons and their axons (Margolis 1972; Monti Graziadei et al. 1977), followed by Cy3-labeled goat anti-goat IgG (1:500, Jackson Immunoresearch), to verify the efficacy of the zinc sulfate lesions.

Cell counts, volume measurements, and density estimates

Image stacks were imported into the confocal module of Neurolucida software (MBF Bioscience Inc., Williston, VT) installed on a PC, and optical disector methods (Sterio 1984; West et al. 1991), modified for confocal microscopy (Parrish-Aungst et al. 2007), were used to quantify labeled cells. Briefly, labeled cell bodies were counted when they first appeared to have a solid perimeter in the image stack, as long as they did not intersect the top of the tissue section (lookup optical section) or the forbidden lines, the latter of which consisted of the mitral cell layer (MCL) and top edge of the image frame. A grid of 25-μm squares was overlaid on the image stack and used to calculate the reference volume. Cells in the most superficial portion of the EPL, at the GL-EPL border, were considered to lie within the EPL, rather than within the GL, if they were surrounded by the dense meshwork of GAD65-GFP processes that characterize this region (see Figure 1f and Supplementary Figure 1c). This definition of the GL-EPL boundary is consistent with our previous anatomical studies and electrophysiological recordings, showing that the most superficial portion of the mouse EPL contains the highest density of EPL interneurons and tufted cells (Hamilton and Coppola 2003; Hamilton et al. 2005; Hamilton KA, unpublished data). However, this definition differed from our recent study in which this region was quantified along with the GL (Parrish-Aungst et al. 2007).

The low-magnification images of the sections were also imported into Neurolucida. Areas of the right OB and EPL were determined by outlining the boundaries using the computer mouse, and the OB and EPL volumes were estimated using the Cavaleri method; the cell counts, numbers of squares counted, and areas were used to estimate numbers of GAD65-GFP, GluR1-IR and PV-IR neurons, and total numbers of Sytox Orange–labeled cells of all types, within the EPL of each right OB. Cell densities were determined by dividing raw cell counts by the counting frame volume.

Amino cupric silver staining

OB sections from another study (Kim et al. 2006) were used to identify degenerating neurons within the EPL, GL, and MCL + GCL. The MCL was combined with the GCL because it contains large numbers of superficial granule cells (Frazier and Brunjes 1988), which have properties distinct from those of deep granule cells (Heinbockel et al. 2007). Four zinc sulfate–treated CD-1 mice were anesthetized and perfused as described above, at 3 or 7 days following treatment, and the brains were shipped in fixative for histological processing (Neuroscience Associates, Knoxville, TN) using the de Olmos amino cupric silver staining method (de Olmos et al. 1994; Switzer 2000). Coronal sections (35 μm) were silver stained, counterstained with Neutral Red, and mounted on slides. Preliminary examination of the sections revealed no detectable differences in staining between animals perfused at the 2 time points, so they were combined for statistical comparisons. Images (1200 × 1600 pixels) of all sections through the right OBs were obtained using a color camera (Optronics Microfire, Goleta, CA), and silver-stained cell bodies were counted if they did not intersect the top or left edges of the image frame. The percentage of cells stained in the EPL of the zinc sulfate–treated mice was compared with the percentages seen in the other layers; total cell numbers were not calculated because a complete set of sections was not available for determining the EPL volume. Two PBS-treated CD-1 mice were also perfused as described above to permit qualitative comparison of the staining patterns with results of previous studies.

Statistical analysis and figures

Estimated numbers of labeled cells in the EPL of the right OBs of zinc sulfate– and PBS-treated animals were compared using *t*-tests (SigmaStat, Systat Software, San José, CA). Cell densities were compared using Mann–Whitney rank sum tests. Percentages of degenerating cells were transformed to permit parametric testing and compared using *t*-tests. *P* values <0.05 were considered significant.

The images shown are extended focus single-wavelength or merged views through the entire medial EPL obtained using Olympus FluoView or Zeiss LSM confocal software or using the confocal plug-in module of Neurolucida. Figures were assembled into montages, labeled, and the contrast and brightness of the image groups adjusted in Photoshop CS (Adobe Systems Inc., San José, CA).

Results

Zinc sulfate treatment reduces the adult mouse EPL volume and neuronal staining

Consistent with previous reports (Margolis et al. 1974), zinc sulfate–treated mice had significantly smaller OBs than PBS-treated mice (right bulb: 4.51 ± 0.52 [mean ± standard error of the mean] mm^3, $N = 6$ lesion vs. 6.93 ± 0.76 mm^3, $N = 7$ control, $P = 0.02$; see Supplementary Figure 1). Although not evident in all sections, the EPL of the zinc sulfate–treated mice was also significantly smaller (right EPL: 1 ± 0.11 mm^3, $N = 6$ lesion vs. 1.52 ± 0.15 mm^3, $N = 7$ control, $P = 0.02$). The OB and EPL volumes of the PBS-treated mice closely resembled our previous measurements obtained from untreated mice (bulb: 7.53 ± 0.43 mm^2, EPL: 1.41 ± 0.10 mm^2; Parrish-Aungst et al. 2007), indicating that PBS treatment had little if any effect. By contrast, the ~35% reduction in OB and EPL volumes of the zinc sulfate–treated mice indicates that zinc sulfate treatment significantly reduced sensory input from the olfactory epithelium. This was confirmed by examining immunoreactivity for olfactory marker protein in the GL, which was greatly reduced (Supplementary Figure 1d), as also observed previously (Baker et al. 1988).

The reduction in EPL volume of the zinc sulfate–treated mice was accompanied by reduced labeling of neuronal somata in the EPL. As can be seen by comparing Figure 1a and e, immunoreactivity of cell bodies for GluR1 was noticeably reduced. The small soma sizes and labeled varicose processes that emanated from many of the labeled cell bodies indicated

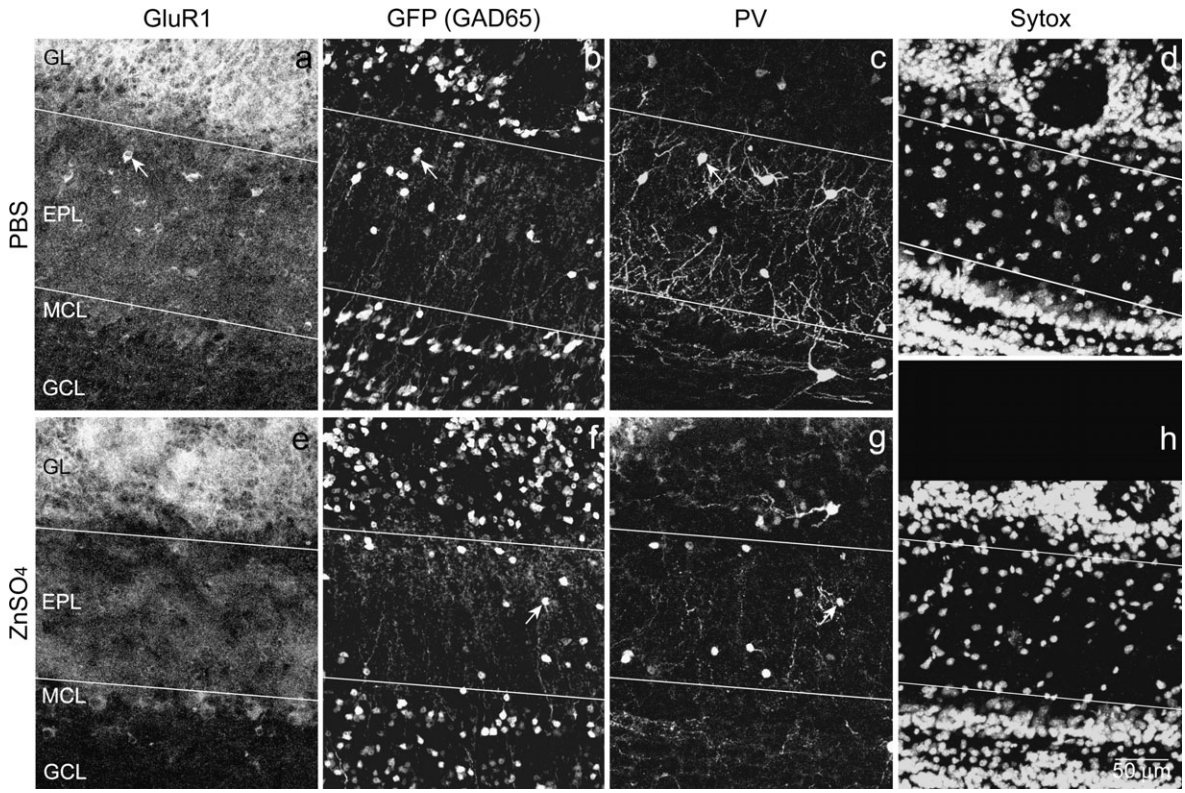

Figure 1 GluR1-IR of neuronal cell bodies was weaker in the EPL of GAD65-GFP transgenic mice treated with zinc sulfate **(e)** than in the EPL of mice treated with PBS **(a)**. By contrast, fluorescence of GFP-labeled neuronal cell bodies **(b** and **f)** and of PV-IR neuronal cell bodies **(c** and **g)** did not appear to be strongly affected. Arrows and arrowheads indicate double- and triple-labeled cell bodies in single sections exhibiting all 3 markers. Note that in zinc sulfate–treated mice, more GAD65-GFP neuronal cell bodies were located in the superficial portion of the EPL, near the GL; this region has the highest density of both EPL interneurons and tufted cells. Similar labeling of cell bodies of all types was observed in sections from the zinc sulfate– and PBS-treated mice stained with Sytox Orange **(d** and **h)**. JG, juxtaglomerular region.

that the small GluR1-IR cells were interneurons, as described previously (Petralia and Wenthold 1992; Montague and Greer 1999; Hamilton and Coppola 2003; Hamilton et al. 2005). Larger cell bodies were also observed, which were presumably those of tufted cells and other interneurons (see Numbers of GABAergic interneurons in the EPL). The loss of GluR1-IR appeared to be restricted to the EPL. GluR1 immunoreactivity of cell bodies in the GL did not appear to be affected, whereas immunoreactivity of mitral cell bodies was somewhat enhanced, as also observed following naris occlusion (Figure 1e; Hamilton and Coppola 2003).

As can be seen by comparing Figure 1b and f, fluorescence of GAD65-GFP cell bodies was generally similar in both zinc sulfate– and PBS-treated mice. In the zinc sulfate–treated mice, however, a higher proportion of the GAD65-GFP cell bodies appeared to be located in the superficial EPL, and there was a small reduction in total cell numbers (see Zinc sulfate treatment reduces numbers and density of GluR1-IR cell bodies in the adult mouse EPL). As mentioned above, the superficial EPL also exhibited a higher density of GFP-labeled processes (e.g., Figure 1f and Supplementary Figure 1c). These observations suggest that zinc sulfate treatment resulted in compaction of the most superficial portion of the EPL. This is noteworthy because different mitral/tufted cell subtypes occur within and/or extend lateral dendrites into the superficial versus deep halves of the layer (reviewed in Ennis et al. 2007; see Discussion).

Although reduced labeling of rat PV-IR cells has been observed following neonatal naris occlusion (Philpot, Foster, et al. 1997), labeling of PV-IR cell bodies was not noticeably altered in the zinc sulfate–treated mice (cf. Figure 1c,g). The PV-IR cells resembled the multipolar interneurons described previously (Kosaka et al. 1994).

Zinc sulfate treatment reduces numbers and density of GluR1-IR cell bodies in the adult mouse EPL

The qualitative difference in GluR1 labeling described above was supported by quantitative differences in numbers of GluR1-IR cell bodies. As shown in Figure 2, the zinc sulfate–treated mice had significantly fewer (34%) GluR1-IR cells ($52.6 \pm 6.2 \times 10^3$, $N = 5$ lesion vs. $155.4 \pm 12.7 \times 10^3$, $N = 5$ control, $P < 0.001$) than the PBS-treated mice. They also had significantly fewer (64%) GAD65-GFP cells ($97.8 \pm 8.1 \times 10^3$, $N = 5$ lesion vs.$152 \pm 13.3 \times 10^3$ $N = 7$ control, $P = 0.007$). In addition, the zinc sulfate–treated mice had significantly fewer GluR1-IR cells that were GAD65-GFP positive ($11.5 \pm 3.0 \times 10^3$, $N = 5$ lesion vs. $53.1 \pm 5.0 \times 10^3$, $N = 5$ control, $P = 0.008$). Numbers of cells that were triple labeled for GluR1, GAD65-GFP, and PV ($14.3 \pm 0.8 \times 10^3$, $N = 5$ lesion vs. $35.5 \pm 2.3 \times 10^3$, $N = 5$ control, $P < 0.001$) also differed significantly, even though total numbers of PV-IR labeled cells did not differ ($27.8 \pm 8.9 \times 10^{-3}$, $N = 5$ lesion vs. $50.2 \pm 4 \times 10^3$, $N = 5$ control, $P = 0.05$). Densities of labeled cell bodies, in addition to their numbers, were also reduced. Densities of GluR1-IR cell bodies, GluR1-IR plus GAD65-GFP cell bodies, and GluR1-IR plus GAD65-GFP plus PV cell bodies were lower in the zinc sulfate–treated mice ($P \leq 0.004$ for all); densities of single-labeled GAD65-GFP and PV-IR cell bodies did not differ, however ($P \geq 0.28$). The reduced density of GluR1 cell bodies was similar to that observed following neonatal naris occlusion (Hamilton and Coppola 2003). The reduction in total numbers of GAD65-GFP and PV-IR cells was also similar to reductions seen following neonatal sensory deprivation; for example, dark-rearing reduces GAD65 levels in the mouse retina (Lee et al. 2006), and neonatal olfactory deprivation reduces PV-IR in the rat EPL (Philpot, Lim, et al. 1997). However, it should be noted that in the present study, the GluR1 phenotype was much more strongly affected by zinc sulfate treatment than expression of either the GAD65 transgene or immunoreactivity for PV. The number of GluR1-IR cells observed in the zinc sulfate–treated mice was approximately half the number of GAD65-GFP cells, whereas approximately equal numbers were observed in the PBS-treated mice. The number of PV-IR cells was ~30% of the number of GluR1-IR cells in both treatment groups (zinc sulfate 28%; PBS 33%).

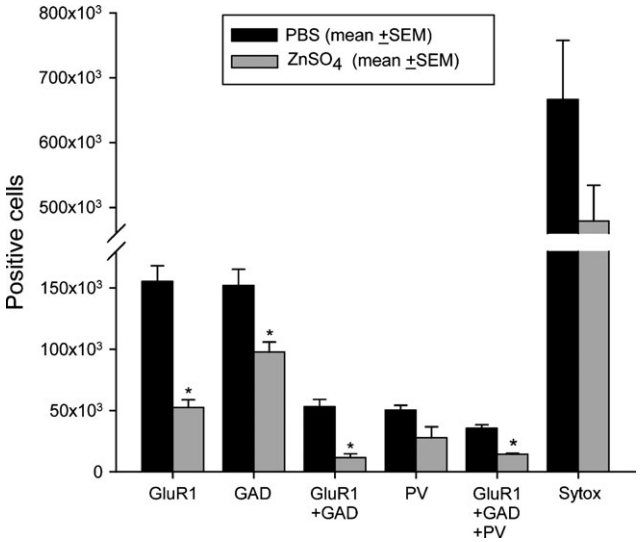

Figure 2 Fewer GluR1-IR, GAD65-GFP, and double-labeled cell bodies occurred in the EPL of zinc sulfate–treated than PBS-treated mice (*, *t*-test $P < 0.05$). Fewer PV-IR neurons also occurred, but the difference was not significant. However, the number of cells that were triple labeled for GluR1, GAD65-GFP, and PV were reduced. Changes in cell densities also occurred (see text).

Zinc sulfate treatment does not significantly reduce total cell numbers within the EPL

As shown in Figure 1d,h, staining of the nuclei of neurons, glia, and other nonneural cells with Sytox Orange did not differ noticeably between the zinc sulfate– and PBS-treated mice. As shown in Figure 2, the EPL of zinc sulfate–treated mice had 72% as many Sytox Orange–stained cells as the EPL of PBS-treated mice (479.1 ± 55.2, $N = 6$ lesion vs. $666.5 \pm 91 \times 10^3$, $N = 7$ control), but this difference was not significant

($P = 0.12$). Density of Sytox Orange–stained cells also did not differ significantly ($P = 0.63$). In both the zinc sulfate– and PBS-treated mice, ~30% of the Sytox Orange–labeled cells expressed GAD65-GFP (29% and 26%, respectively). The other ~70% were presumably tufted cells, nonneural cells, and interneurons that did not express GAD65 (see Numbers of GABAergic interneurons in the EPL). Attempts to differentiate neuronal from nonneural cells using the neuronal antigen marker neuron-specific nuclear protein (NeuN) were only partially successful because NeuN fails to label many GABAergic interneurons in the superficial layers of the mouse OB (Panzanelli et al. 2007; Parrish-Aungst et al. 2007).

It should be noted here that numbers of GAD65-GFP and PV-IR cell bodies in the EPL of the PBS-treated mice was ~4 times higher than reported previously for the same transgenic mouse strain (Parrish-Aungst et al. 2007). The total number of cell bodies labeled with Sytox Orange was also higher than the total number of cell bodies labeled with Sytox Green in that study. These apparent discrepancies are likely due to the fact that the EPL border with the GL region was counted with the EPL in the present study and with the GL in the previous study (see Experimental Procedures). Although this boundary region represents a small portion of the total EPL volume, it typically has a higher interneuron density than deeper portions of the EPL (see Figure 1).

Numbers of GABAergic interneurons in the EPL

As shown in Figure 2, in PBS-treated mice, 23% of the GluR1-IR cells and 10% of the PV-IR cells also expressed GAD65-GFP (53.1×10^3 and 4.8×10^3, respectively). This suggests that the EPL contains ~60×10^3 interneurons. Because many GluR1-IR EPL cells and all PV-IR cells are thought to be interneurons, and EPL interneurons are thought to be inhibitory, the question arises as to why more of the 155×10^3 GluR1-IR cells did not co-express GAD65-GFP? We have previously estimated that 14% of EPL neurons express the 67-kDa isoform of GAD and that 6% of EPL neurons express calretinin but not PV or GAD (Parrish-Aungst et al. 2007). Thus, an additional 33×10^3 GluR1-IR cells could be interneurons that did not express GAD65-GFP. Another 7×10^3 of the GluR1-IR cells were PV-IR interneurons that did not express GAD65-GFP, bringing the total number of GluR1-IR interneurons to ~100×10^3. The other ~55×10^3 GluR1-IR cells were presumably mostly tufted cells, although this number could also have included small numbers of other interneurons that did not express detectable levels of any of the interneuron markers used. For example, the rat EPL contains some vasoactive intestinal polypeptide-IR and calbindin-IR interneurons (Gall et al. 1986; Celio 1990; Briñón et al. 1992), and the mouse EPL contains rare neurocalcin-IR interneurons (Briñón et al. 1998; Murias et al. 2007). We have previously estimated that the tufted cells and GAD-negative interneurons of the mouse EPL constitute ~30% of EPL cells (Parrish-Aungst et al. 2007), which agrees well with the 36% GluR1-IR "tufted" cell figure derived here.

The EPL of zinc sulfate–treated animals contains few degenerating cells relative to other OB layers

Figure 3 shows the percentages of degenerating cells stained in different OB layers using the amino cupric silver staining method. In both the zinc sulfate– and PBS-treated animals, the total number of degenerating cells was a small fraction of all OB cells. However, in the zinc sulfate–treated animals, higher proportions of the degenerating cells occurred in the GL (27%) and MCL + GCL (64%) than in the EPL (9%, $P < 0.001$). The average number of degenerating cells seen in sections through the EPL of the 4 zinc sulfate–treated animals (8, range 6–13) did not appear to differ from the average seen in the EPL of the 2 PBS-treated animals (9, range 2–14). By contrast, numbers of degenerating cells seemed to increase in the GL (26 vs. 10) and MCL + GCL (61 vs. 17). These comparisons support previous quantitative results from naris occlusion studies showing that olfactory deprivation in adulthood results in cell loss primarily from the GL and MCL + GCL; most of the loss is of interneurons (and progenitors) from the GCL, however (Corotto et al. 1994; Najbauer and Leon 1995; Fiske and Brunjes 2001; Tyler et al. 2007). Almost all tufted and mitral cells are generated prenatally (Hinds 1967; Bayer 1983). It is, therefore, unlikely that tufted cell death contributed significantly to the discrepancy between the reduction in GluR1-IR cell bodies and small number of degenerating cells seen here. Thus, the reduction in GluR1-IR was most likely due to downregulation of GluR1 expression, rather than to widespread neuronal loss.

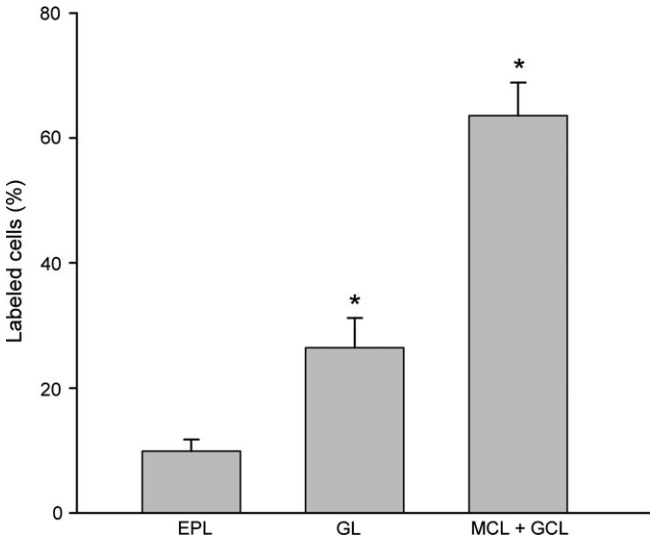

Figure 3 Following zinc sulfate treatment, fewer degenerating cells were observed in the EPL than GL or MCL + GCL, as revealed by amino cupric silver staining. Only 9% of the labeled cells occurred in the EPL. Significantly higher percentages occurred in the GL (27%) and MCL + GCL (64%, $P < 0.001$).

Discussion

Our results indicate that both the number and density of GluR1-IR cell bodies are reduced in the EPL following loss of olfactory input to the adult OB. The GluR1-IR cell population also loses some expression of the 65-kDa isozyme of GAD and immunoreactivity for PV. Because most of these cells are interneurons that do not receive direct olfactory input, but instead receive input via mitral/tufted cells, our results suggest that expression of multiple neuronal markers in the adult EPL can be transsynaptically regulated by olfactory stimulation. The large, 66%, reduction in numbers of EPL cell bodies that are immunoreactive for GluR1 is similar to the dramatic reduction observed following neonatal naris occlusion (Hamilton and Coppola 2003). In the present study, the reduction in GluR1 labeling was shown to be significantly larger than the reduction in other interneuron markers (GAD65 and PV). This suggests that GluR1 expression by both interneurons and tufted cells is sensitive to olfactory input. We have previously reported that expression of the *N*-methyl-D-aspartic acid (NMDA) receptor NR2B subunit in the piriform cortex is also reduced following adult olfactory deafferentation (Kim et al. 2006). Neuronal excitation via both AMPA and NMDA receptors could, therefore, be affected at 2 different levels of olfactory processing.

The EPL contains significant numbers of superficial and middle tufted cells, as well as a small number of deep tufted cells. It is estimated that the total number of these tufted cells, plus external tufted cells, could be as high as twice the number of mitral cells (Allison 1953; Shepherd et al. 2004). Although several staining methods label some EPL tufted cells (e.g., cholecystokinin, Seroogy et al. 1985; T-box transcription factors, Bulfone et al. 1995; Faedo et al. 2002; Yoshihara et al. 2005; Allen et al. 2007), these methods do label all tufted cell subtypes. Direct evidence for loss of GluR1-IR by tufted cells is, therefore, lacking. However, because the EPL contains large numbers of tufted cells and few interneurons that express markers other than GAD65 and PV, it is likely that the reduced numbers of GluR1-IR cell bodies seen here resulted from loss of GluR1 expression by both tufted cells and interneurons.

In hippocampal pyramidal cells, GluR1 is required to maintain the pool of nonsynaptic AMPA receptors, which are recruited to the postsynaptic membrane as a result of high-frequency stimulation (Hayashi et al. 2000; Shi et al. 2001; Esteban et al. 2003; Lee et al. 2003; Boehm et al. 2006). Mice lacking GluR1 and mice with mutated GluR1 subunits exhibit deficits in long-term potentiation and in spatial memory (Zamanillo et al. 1999; Reisel et al. 2002; Lee et al. 2003). The loss of GluR1-IR observed in this study could, therefore, represent a loss of somatic extrasynaptic receptors. Studies of hippocampal pyramidal cells have also shown that loss of GluR1 from cell bodies can be accompanied by gain of GluR1-containing AMPA receptors at dendritic synapses. In cultured cells, extrasynaptic AMPA receptors can rapidly be inserted into the membrane and travel to dendritic sites (Adesnik et al. 2005). Blocking activity can enhance the synaptic insertion of homomeric GluR1 AMPA receptors, perhaps as a means of restoring the neuronal excitatory set point (Turrigiano and Nelson 2000; Thiagarajan et al. 2005). If olfactory deafferentation has a similar effect on dendritic AMPA receptors of EPL interneurons, then the distribution of GluR1 in the OB, but not its overall expression, might be altered. There is evidence that the distribution of GluR1 immunoreactivity is altered following olfactory deprivation; it appears to be enhanced in the GL following naris occlusion (Tyler et al. 2007) and in mitral cell bodies as a result of both deafferentation and naris occlusion (Figure 1e; Fig. 1C in Hamilton and Coppola 2003). GluR1 expression by the entire OB is unaffected by olfactory deafferentation, however, as demonstrated by reverse transcriptase–polymerase chain reaction (Kim et al. 2006).

In the present study, olfactory deafferentation resulted in an apparent compaction of the superficial EPL, as indicated by GAD65-GFP fluorescence. Similar changes in the stratification of this layer have been observed following neonatal olfactory deprivation (e.g., Couper Leo et al. 2000). It is, therefore, important to note that cell bodies and lateral dendrites of all superficial tufted cells and most middle tufted cells are restricted to the superficial half of the EPL (Mori et al. 1983; Scott and Harrison 1987). Apical dendrites of different granule cell subtypes also project within the superficial versus deep portions of the EPL, and the 2 regions exhibit different staining intensities for a host of substances (reviewed in Ennis et al. 2007). Thus, the superficial and deep portions of the EPL likely perform different functions in regulating mitral/tufted cell output from the OB. Modeling of field potential recordings suggests that the tufted cells of the EPL generate a significant portion (39%) of spontaneous OB activity (Karnup et al. 2006). Other recordings suggest that superficially located tufted cells may be largely responsible for this activity. These cells are more responsive to ON stimulation than deep tufted cells (Schneider and Scott 1983; Wellis et al. 1989; Ezeh et al. 1993), and they exhibit prolonged excitation in response to odor stimulation (Luo and Katz 2001). Thus, superficially located tufted cells appear to be more sensitive and responsive to olfactory stimulation than deep tufted cells and mitral cells. The compaction of the superficial EPL that occurs following olfactory deafferentation could, therefore, reflect effects of reduced olfactory input specifically upon these more sensitive/responsive tufted cell subtypes. If EPL interneurons receive most of their excitatory synaptic input from these tufted cell subtypes, via GluR1-containing AMPA receptors, then this might be why the GluR1-IR of EPL interneurons is so strongly affected by olfactory deafferentation and deprivation.

We have previously shown that EPL interneurons receive large, spontaneous, high-frequency excitatory postsynaptic potential barrages that are mediated by AMPA/kainate

receptors (Hamilton et al. 2005). Mitral/tufted cells are glutamatergic, and serial section reconstruction studies have shown that they form excitatory synapses onto PV-IR EPL interneurons, which form inhibitory synapses onto mitral/tufted cells, 30–50% of which are reciprocal (Toida et al. 1996; Crespo et al. 2001). EPL interneurons, therefore, appear to receive robust, ongoing, AMPA/kainate receptor–mediated glutamatergic excitation from mitral/tufted cells, even in the absence of olfactory stimulation, and they in turn appear to inhibit mitral/tufted cells within the EPL. If loss of GluR1-IR by cell bodies of EPL interneurons occurs in concert with insertion of additional AMPA receptors at their mitral/tufted cell synapses, then the reduced GluR1-IR of the interneuron cell bodies could be indicative of a compensatory mechanism that serves to restore the normal, spontaneous level of mitral/tufted cell inhibition. Naris occlusion studies have shown that reduced olfactory input to the developing OB decreases mitral/tufted cell spontaneous activity and increases mitral/tufted cell inhibition (Guthrie et al. 1990; Wilson and Wood 1992; Philpot, Foster, et al. 1997). This appears to be due to increased amplitude of synaptic currents mediated by both AMPA and NMDA receptors, which results in enhanced inhibition from periglomerular cells and granule cells (Saghatelyan et al. 2005; Tyler et al. 2007). Results of the present study suggest that GluR1-containing AMPA receptors of EPL interneurons might play a heretofore unappreciated role in regulating mitral/tufted cell activity, within the OB EPL.

Supplementary material

Supplementary material can be found at http://www.chemse.oxfordjournals.org.

Funding

National Institutes of Health (DC03112 to F.L.M, DC005676 to Michael T. Shipley, DC05739 to A.C.P.), State of Maryland MSCRFE0239 (to A.C.P.), and the Biomedical Research Foundation of Northwest Louisiana (to K.A.H.).

Acknowledgements

We thank Wanda Green for assistance with degenerating cell counts and Dr Hyun Hee Kim for helpful discussions of this work.

References

Adesnik H, Nicoll RA, England PM. 2005. Photoinactivation of native AMPA receptors reveals their real-time trafficking. Neuron. 48:977–985.

Allen ZJ, Waclaw RR, Colbert MC, Campbell K. 2007. Molecular identity of olfactory bulb interneurons: transcriptional codes of periglomerular neuron subtypes. J Mol Histol. doi 10.1007/510735-007-9115-4.

Allison AC. 1953. The morphology of the olfactory system in the vertebrates. Biol Rev. 28:195–255.

Aroniadou-Anderjaska V, Ennis M, Shipley MT. 1997. Glomerular synaptic responses to olfactory nerve input in rat olfactory bulb slices. Neuroscience. 79:425–434.

Baker H. 1990. Unilateral, neonatal olfactory deprivation alters tyrosine hydroxylase expression but not aromatic amino acid decarboxylase or GABA immunoreactivity. Neuroscience. 36:761–771.

Baker H, Kawano T, Albert V, Joh TH, Reis DJ, Margolis FL. 1984. Olfactory bulb dopamine neurons survive deafferentation-induced loss of tyrosine hydroxylase. Neuroscience. 11:605–615.

Baker H, Towle AC, Margolis FL. 1988. Differential afferent regulation of dopaminergic and GABAergic neurons in the mouse main olfactory bulb. Brain Res. 450:69–80.

Bayer SA. 1983. ^{3}H-Thymidine-autoradiographic studies of neurogenesis in the rat olfactory bulb. Exp Brain Res. 50:329–340.

Boehm J, Kang M-G, Johnson RC, Esteban J, Huganir RL, Malinow R. 2006. Synaptic incorporation of AMPA receptors during LTP is controlled by a PKC phosphorylation site on GluR1. Neuron. 51:213–225.

Bredt DS, Nicholl RA. 2003. AMPA receptor trafficking at excitatory synapses. Neuron. 40:361–379.

Briñón JG, Alonso JR, Arévalo R, Garcia-Ojeda E, Lara J, Aijón J. 1992. Calbindin D-28k-positive neurons in the rat olfactory bulb. An immunohistochemical study. Cell Tissue Res. 269:289–297.

Briñón JG, Arévalo R, Crespo C, Bravo IG, Okazaki K, Hidaka H, Aijón J, Alonso JR. 1998. Neurocalcin immunoreactivity in the rat main olfactory bulb. Brain Res. 797:204–214.

Brunjes PC. 1994. Unilateral naris closure and olfactory system development. Brain Res Rev. 19:146–160.

Bulfone A, Smiga SM, Shimamura K, Petersen A, Puelles L, Rubenstein JLR. 1995. T-Brain-1: a homolog of Brachyury whose expression defines molecularly distinct domains within the cerebral cortex. Neuron. 15: 63–78.

Burd GD. 1993. Morphological study of the effects of intranasal zinc sulfate irrigation on the mouse olfactory epithelium and olfactory bulb. Microsc Res Tech. 24:195–213.

Celio MR. 1990. Calbindin D-28k and parvalbumin in the rat nervous system. Neuroscience. 35:375–475.

Chen WR, Shepherd GM. 1997. Membrane and synaptic properties of mitral cells in slices of rat olfactory bulb. Brain Res. 745:189–196.

Corotto FS, Henegar JR, Maruniak JA. 1994. Odor deprivation leads to reduced neurogenesis and reduced neuronal survival in the olfactory bulb of the adult mouse. Neuroscience. 61:739–744.

Couper Leo JM, Devine AH, Brunjes PC. 2000. Focal denervation alters cellular phenotypes and survival in the rat olfactory bulb: a developmental analysis. J Comp Neurol. 425:409–421.

Crespo C, Blasco-Ibáñez JM, Marqués-Mari AI, Martínez-Guijarro FJ. 2001. Parvalbumin-containing interneurons do not innervate granule cells in the olfactory bulb. Neuroreport. 12:2553–2556.

De Marchis S, Bovetti S, Carletti B, Hsieh Y-C, Garzotto D, Peretto P, Fasolo A, Puche AC, Rossi F. 2007. Generation of distinct types of periglomerular olfactory bulb interneurons during development and in adult mice: implications for intrinsic properties of the subventricular zone progenitor population. J Neurosci. 27:657–664.

De Marchis S, Fasolo A, Shipley M, Puche A. 2001. Unique neuronal tracers show migration and differentiation of SVZ progenitors in organotypic slices. J Neurobiol. 49:326–338.

de Olmos JS, Beltramino CA, de Olmos de Lorenzo S. 1994. Use of an amino-cupric silver technique for detection of early and semiacute neuronal degeneration caused by neurotoxicants, hypoxia, and physical trauma. Neurotoxicol Teratol. 16:545–561.

Ennis M, Hamilton KA, Hayar A. 2007. Neurochemistry of the main olfactory system. In: Lajtha A, Johnson D, editors. Handbook of neurochemistry and molecular neurobiology 3/e. Chapter 6. Sensory neurochemistry. Vol. 20. New York: Springer.

Ennis M, Zimmer LA, Shipley MT. 1996. Olfactory nerve stimulation activates rat mitral cells via NMDA and non-NMDA receptors in vitro. Neuroreport. 7:989–992.

Erdélyi F, Sekerkova G, Katarova Z, Hájos N, Palhalmi J, Freund TF, Mugnaini E, Szabó G. 2002. GAD65-GFP transgenic mice expressing GFP in the GABAergic nervous system. FENS Abstr. 1:AO11–AO13.

Esteban JA, Shi S-H, Wilson C, Nuriya M, Huganir RL, Malinow R. 2003. PKA phosphorylation of AMPA receptor subunits controls synaptic trafficking underlying plasticity. Nat Neurosci. 6:136–143.

Ezeh PI, Wellis DP, Scott JW. 1993. Organization of inhibition in the rat olfactory bulb external plexiform layer. J Neurophysiol. 70:263–274.

Faedo A, Ficara F, Ghiani M, Aiuti A, Rubenstein JLR, Bulfone A. 2002. Developmental expression of the T-box transcription factor T-bet/Tbx21 during mouse embryogenesis. Mech Dev. 116:157–160.

Fiske BK, Brunjes PC. 2001. Cell death in the developing and sensory-deprived rat olfactory bulb. J Comp Neurol. 431:311–319.

Frazier LL, Brunjes PC. 1988. Unilateral odor deprivation: early postnatal changes in olfactory bulb cell density and number. J Comp Neurol. 269:355–370.

Frazier-Cierpial L, Brunjes PC. 1989. Early postnatal cellular proliferation and survival in the olfactory bulb and rostral migratory stream of normal and unilaterally odor-deprived rats. J Comp Neurol. 289:481–492.

Gall C, Seroogy KM, Brecha N. 1986. Distribution of VIP- and NPY-like immunoreactivities in the rat main olfactory bulb. Brain Res. 374:389–394.

Giustetto M, Bovolin P, Fasolo A, Bonino M, Cantino D, Sassoè-Pognetto M. 1997. Glutamate receptors in the olfactory bulb synaptic circuitry: heterogeneity and synaptic localization of *N*-methyl-D-aspartate receptor subunit 1 and AMPA receptor subunit 1. Neuroscience. 76:787–798.

Guthrie KM, Wilson DA, Leon M. 1990. Early unilateral deprivation modifies olfactory bulb function. J Neurosci. 10:3402–3412.

Hamilton KA, Coppola DM. 2003. Distribution of GluR1 is altered in the olfactory bulb following neonatal naris occlusion. J Neurobiol. 54:326–336.

Hamilton KA, Heinbockel T, Ennis M, Szabó G, Erdélyi F, Hayar A. 2005. Properties of external plexiform layer interneurons in mouse olfactory bulb slices. Neuroscience. 133:819–829.

Harding JW, Getchell TV, Margolis FL. 1978. Denervation of the primary olfactory pathway in mice. V. Long-term effect of intranasal $ZnSO_4$ irrigation on behavior, biochemistry and morphology. Brain Res. 140:271–285.

Hayashi Y, Shi S-H, Esteban JA, Piccini A, Poncer J-C, Malinow R. 2000. Driving AMPA receptors into synapses by LTP and CamKII: requirement for GluR1 and PDZ domain interaction. Science. 287:2262–2267.

Heinbockel T, Hamilton KA, Ennis M. 2007. Group I metabotropic glutamate receptors are differentially expressed by two populations of olfactory bulb granule cells. J Neurophysiol. 97:3136–3141.

Hinds JW. 1967. Autoradiographic study of histogenesis in the mouse olfactory bulb. II. Cell proliferation and migration. J Comp Neurol. 134:305–322.

Kaplan MS, McNelly NA, Hinds JW. 1985. Population dynamics of adult-formed granule neurons of the rat olfactory bulb. J Comp Neurol. 239:117–125.

Karnup SV, Hayar A, Shipley MT, Kurnikova MG. 2006. Spontaneous field potentials in the glomeruli of the olfactory bulb: the leading role of juxtaglomerular cells. Neuroscience. 142:203–221.

Kato T, Yokouchi K, Kawagishi K, Fukushima N, Miwa T, Moriizumi T. 2000. Fate of newly formed periglomerular cells in the olfactory bulb. Acta Otlaryngol. 120:876–879.

Kawano T, Margolis FL. 1982. Transsynaptic regulation of olfactory bulb catecholamines in mice and rats. J Neurochem. 39:342–348.

Kim HH, Puche AC, Margolis FL. 2006. Odorant deprivation reversibly modulates transsynaptic changes in the NR2B-mediated CREB pathway in mouse piriform cortex. J Neurosci. 26:9548–9559.

Kosaka K, Heizmann CW, Kosaka T. 1994a. Calcium-binding protein parvalbumin-immunoreactive neurons in the rat olfactory bulb. 1. Distribution and structural features in adult rat. Exp Brain Res. 99:191–204.

Kosaka K, Heizmann CW, Kosaka T. 1994b. Calcium-binding protein parvalbumin-immunoreactive neurons in the rat olfactory bulb. 2. Postnatal development. Exp Brain Res. 99:205–213.

Kosaka T, Kosaka K, Hama K, Wu J-Y, Nagatsu I. 1987. Differential effect of functional olfactory deprivation on the GABAergic and catecholaminergic traits in the rat main olfactory bulb. Brain Res. 413:197–203.

Lee E-J, Gibo TL, Grzywacz NM. 2006. Dark-rearing-induced reduction of GABA and GAD and prevention of the effect by BDNF in the mouse retina. Eur J Neurosci. 24:2118–2134.

Lee H-K, Takamiya K, Han J-S, Man H, Kim C-H, Rumbagh G, Yu S, Ding L, He C, Pertalia RS, et al. 2003. Phosphorylation of the AMPA receptor GluR1 subunit is required for synaptic plasticity and retention of spatial memory. Cell. 112:631–643.

Lois C, Alvarez-Buylla A. 1994. Long-distance neuronal migration in the adult mammalian brain. Science. 264:1145–1148.

López-Bendito G, Sturgess K, Erdélyi F, Szabó G, Molnár Z, Paulsen O. 2004. Preferential origin and layer destination of GAD65-GFP cortical interneurons. Cereb Cortex. 14:1122–1133.

Luo M, Katz L. 2001. Response correlation maps of neurons in the mammalian olfactory bulb. Neuron. 32:1165–1179.

Luskin MB. 1993. Restricted proliferation and migration of postnatally generated neurons derived from the forebrain subventricular zone. Neuron. 11:173–189.

Mandairon N, Sacquet J, Jourdan F, Didier A. 2006. Long-term fate and distribution of newborn cells in the adult mouse olfactory bulb: influences of olfactory deprivation. Neuroscience. 141:443–451.

Margolis FL. 1972. A brain protein unique to the olfactory bulb. Proc Natl Acad Sci USA. 69:1221–1224.

Margolis FL, Roberts N, Ferriero D, Feldman J. 1974. Denervation in the primary olfactory pathway of mice: biochemical and morphological effects. Brain Res. 81:469–483.

Matulionis DH. 1975. Ultrastructural study of mouse olfactory epithelium following destruction by $ZnSO_4$ and its subsequent regeneration. Am J Anat. 142:67–90.

McBride K, Slotnick B, Margolis FL. 2003. Does intranasal application of zinc sulfate produce anosmia in the mouse? An olfactometric and anatomical study. Chem Senses. 28:659–670.

Montague AA, Greer CA. 1999. Differential distribution of ionotropic glutamate receptor subunits in the rat olfactory bulb. J Comp Neurol. 405:233–246.

Monti Graziadei GA, Margolis FL, Harding JW, Graziedei PPC. 1977. Immunocytochemistry of the olfactory marker protein. J Histochem Cytochem. 25:1311–1316.

Mori K, Kishi K, Ojima H. 1983. Distribution of dendrites of mitral, displaced mitral, tufted, and granule cells in the rabbit olfactory bulb. J Comp Neurol. 219:339–355.

Murias AR, Weruaga E, Recio JS, Airado C, Díaz D, Alonso JR. 2007. Distribution of neurocalcin-containing neurons reveals sexual dimorphism in the mouse olfactory bulb. Chem Senses. 32:673–680.

Nadi NS, Head R, Grillo M, Hempstead J, Grannot-Reisfeld N, Margolis FL. 1981. Chemical deafferentation of the olfactory bulb: plasticity of the levels of tyrosine hydroxylase, dopamine, and norepinephrine. Brain Res. 213:365–377.

Najbauer J, Leon M. 1995. Olfactory experience modulates apoptosis in the developing olfactory bulb. Brain Res. 674:245–251.

Ninkovic J, Mori T, Götz M. 2007. Distinct modes of neuron addition in adult mouse neurogenesis. J Neurosci. 27:10906–10911.

Panzanelli P, Fritschy JM, Yanagawa Y, Obata K, Sassoè-Pognetto M. 2007. GABAergic phenotype of periglomerular cells in the rodent olfactory bulb. J Comp Neurol. 502:990–1002.

Parrish-Aungst S, Shipley MT, Erdélyi F, Szabó G, Puche AC. 2007. Quantitative analysis of neuronal diversity in the mouse olfactory bulb. J Comp Neurol. 501:825–836.

Petralia RS, Wenthold RJ. 1992. Light and electron immunocytochemical localization of AMPA-selective glutamate receptors in the rat brain. J Comp Neurol. 318:329–354.

Petreanu L, Alvarez-Buylla A. 2002. Maturation and death of adult-born olfactory bulb granule neurons: role of olfaction. J Neurosci. 22:6106–6113.

Philpot BD, Foster TC, Brunjes PC. 1997. Mitral/tufted cell activity is attenuated and becomes uncoupled from respiration following naris closure. J Neurobiol. 33:374–386.

Philpot BD, Lim JH, Brunjes PC. 1997. Activity-dependent regulation of calcium-binding proteins in the developing rat olfactory bulb. J Comp Neurol. 387:12–26.

Reisel D, Bannerman DM, Schmitt WB, Deacon RMJ, Flint J, Borchardt T, Seeburg PH, Rawlins JNP. 2002. Spatial memory dissociations in mice lacking GluR1. Nat Neurosci. 9:868–873.

Saghatelyan A, Roux P, Migliore M, Rochefort C, Desmaisons D, Charneau P, Shepherd GM, Lledo P-M. 2005. Activity-dependent adjustments of the inhibitory network in the olfactory bulb following early postnatal deprivation. Neuron. 46:103–116.

Saino-Saito S, Sasaki H, Volpe BT, Kobayashi K, Berlin R, Baker H. 2004. Differentiation of the dopaminergic phenotype in the olfactory system of neonatal and adult mice. J Comp Neurol. 479:389–398.

Sassoè-Pognetto M, Ottersen OP. 2000. Organization of ionotropic glutamate receptors at dendrodendritic synapses in the rat olfactory bulb. J Neurosci. 20:2192–2201.

Schneider SP, Scott JW. 1983. Orthodromic response properties of rat olfactory mitral and tufted cells correlate with their projection patterns. J Neurophysiol. 50:358–378.

Scott JW, Harrison TA. 1987. The olfactory bulb: anatomy and physiology. In: Finger TE, Silver WF, editors. Neurobiology of taste and smell. New York: Wiley. p. 151–178.

Seroogy KB, Brecha N, Gall C. 1985. Distribution of cholecystokinin-like immunoreactivity in the rat main olfactory bulb. J Comp Neurol. 238:373–383.

Shepherd GM, Chen WR, Greer CA. 2004. Olfactory bulb. In: Shepherd GM, editor. The synaptic organization of the brain. 5th ed. New York: Oxford University Press. p. 165–216.

Shi S-H, Hayashi Y, Esteban JA, Malinow R. 2001. Subunit-specific rules governing AMPA receptor trafficking to synapses in hippocampal pyramidal neurons. Cell. 105:331–343.

Sprengel R. 2006. Role of AMPA receptors in synaptic plasticity. Cell Tissue Res. 326:447–455.

Sterio DC. 1984. The unbiased estimation of number and sizes of arbitrary particles using the disector. J Microsc. 134:127–136.

Stone DM, Grillo M, Margolis FL, Joh TH, Baker H. 1991. Differential effect of functional olfactory bulb deafferentation on tyrosine hydroxylase and glutamic acid decarboxylase messenger RNA levels in rodent juxtaglomerular neurons. J Comp Neurol. 311:223–233.

Switzer RC III. 2000. Application of silver degeneration stains for neurotoxicity testing. Toxicol Pathol. 28:70–83.

Takei H, Yang JL, ul Quraish A, Kakuta S. 2002. Origin and migration of interneurons of the olfactory bulb in the musk shrew, *Suncus murinus*. Arch Histol Cytol. 65:159–168.

Thiagarajan TC, Lindskog M, Tsien RW. 2005. Adaptation to synaptic inactivity in hippocampal neurons. Neuron. 47:725–737.

Toida K, Kosaka K, Aika Y, Kosaka T. 2000. Chemically defined neuron groups and their subpopulations in the glomerular layer of the rat main olfactory bulb—IV. Intraglomerular synapses of tyrosine hydroxylase-immunoreactive neurons. Neuroscience. 101:11–17.

Toida K, Kosaka K, Heizmann CW, Kosaka T. 1994. Synaptic contacts between mitral/tufted cells and GABAergic neurons containing calcium-binding protein parvalbumin in the rat olfactory bulb, with special reference to reciprocal synapses between them. Brain Res. 650:347–352.

Toida K, Kosaka K, Heizmann CW, Kosaka T. 1996. Electron microscopic serial-sectioning/reconstruction study of parvalbumin-containing neurons in the external plexiform layer of the rat olfactory bulb. Neuroscience. 72:449–466.

Turrigiano GG, Nelson SB. 2000. Hebb and homeostasis in neuronal plasticity. Curr Opin Neurobiol. 10:358–364.

Tyler WJ, Petzold GC, Pal SK, Murthy VN. 2007. Experience-dependent modification of primary sensory synapses in the mammalian olfactory bulb. J Neurosci. 27:9427–9438.

Wellis DP, Scott JW, Harrison TA. 1989. Discrimination among odorants by single neurons of the rat olfactory bulb. J Neurophysiol. 61:1161–1177.

West MJ, Slomianka L, Gundersen HJG. 1991. Unbiased stereological estimation of the total number of neurons in the subdivisions of the rat hippocampus using the optical fractionator. Anat Rec. 231:482–497.

Wichterle H, Turnbull DH, Nery S, Fishell G, Alvarez-Buylla A. 2001. In utero fate mapping reveals distinct migratory pathways and fates of neurons born in the mammalian basal forebrain. Development. 128: 3759–3771.

Wilson DA, Wood JG. 1992. Functional consequences of unilateral olfactory deprivation: time-course and age sensitivity. Neuroscience. 49:183–192.

Yoshihara S, Omichi K, Yanazawa M, Kitamura K, Yoshihara Y. 2005. Arx homeobox gene is essential for development of mouse olfactory system. Development. 132:751–762.

Young KM, Fogarty M, Kessaris N, Richardson WD. 2007. Subventricular zone stem cells are heterogeneous with respect to their embryonic origins and neurogenic fates in the adult olfactory bulb. J Neurosci. 27: 8286–8296.

Zamanillo D, Sprengel R, Hvalby O, Jensen V, Burnashev N, Rozov A, Kaiser KMM, Köster HJ, Borchardt T, Worley P, et al. 1999. Importance of AMPA receptors for hippocampal synaptic plasticity but not for spatial learning. Science. 284:1805–1811.

Accepted November 1, 2007